Proc. Indian Acad. Sci. (Chem. **Sci.),** Vol. **98,** Nos 5 & 6, June **1987,** pp. 453–468.

Solubilization of bilirubin by cholate micelles. Spectroscopic and gel permeation studies

KASTURI LAHIRI PURANAM and P **BALARAM**
Molecular Biophysics Unit, Indian Institute of Science, Bangalore 560 012, India

Abstract. The interactions of bilirubin with bile salts have been studied using fluorescence, circular dichroism and ^{1}H NMR methods. Enhancement of bilirubin fluorescence and induction of optical activity in bilirubin in the presence of cholate has been observed. Fluorescence enhancement is pronounced above the critical micelle concentration, while induced CD bands are detectable even in the premicellar region. Dehydrocholate and deoxycholate did not cause a fluorescence increase, but induced CD bands were observed for bilirubin in these cases. Gel permeation chromatography on Sephadex G-50 yielded a single bilirubin-cholate species at alkaline pH, while two species were obtained at neutral pH. ^{1}H NMR and CD spectral characterizations of these complexes are reported. **A 4:** 1 cholate-bilirubin mixture has been analysed by difference (nuclear Overhauser effect) NOE spectroscopy. Observation of strong, negative NOE, both intermolecular and intramolecular leads to the coeclusion chat specific methyl groups on bilirubin and cholate are proximal in the mixed micelle.

Keywords. Bilirubin; bile salts; micelles; induced circular dichroism; fluorescence; nuclear Overhauser effects.

1. Introduction

An important aspect of biliary physical chemistry is the physical state of organic anions in bile. Bilirubin is one of the most thoroughly studied anions because of its biological and clinical importance. Other anions are drugs and dyes like indocyanine green, bromsulphphthalein, rose bengal etc. Many of these are incorporated into mixed micelles of lipids and bile acids (Bickel and Minder ,1970; Scharschmidt and Schrnid 1978; Reuben *et al* 1982). **A** physical association with lipid micelles helps in the effective excretion of the xenobiotics in bile (Reuben 1984).

Bilirubin **IX** α is the end product of heme degradation in mammals (Brown and Troxler 1982) which has necessarily to be excreted as it serves no useful purpose and is neurotoxic. Bilirubin is practically insoluble under physiological conditions and is transported in blood as the serum albumin complex (Meuwissen and Heirwegh 1982) to the liver, where it undergoes conjugation with glucuronic acid to form the more soluble diglucuronides. In the case of bilirubin, the rate of biliary secretion has been shown to rise with an increase in biliary output of bile salts (Goresky *et al* 1974). The solubility of bilirubin has been found to be enhanced in the presence of bile salts (Carey and Koretsky 1979; Ostrow and Celic 1984). Bilirubin is therefore thought to be associated with mixed micelles of lecithin and bile salts. However, structural details of such an interaction between bilirubin **and**

bile salts are lacking and that has prompted us to undertake a spectroscopic investigation of this system. This report summarizes fluorescence, circular dichroism (CD), gel permeation and ^{1}H NMR studies of bilirubin-bile salt complexes.

2. Materials and methods

Bilirubin obtained from Sigma Chemical Co. was purified according to the procedure of McDonagh and Assisi (1972). Cholic acid, dehydrocholic acid and sodium deoxycholate were also from Sigma. Both cholic acid and dehydrocholic acid were converted into their sodium salts by adding a molar equivalent of sodium hydroxide and subsequent lyophilization.

Aqueous stock solutions of bilirubin were prepared using sodium hydroxide for complete dissolution. The concentration of such stock solutions was determined using ε_{438} = 47,000 $M^{-1}cm^{-1}$ (Carey and Koretsky 1979). The solutions were used within two to three hours of preparation. Samples containing bilirubin and cholate for ^{1}H NMR studies were made by addition of solid bilirubin to the cholate solution in D_2O and then increasing the pD of the solution to $\backsim$ 10·5 using NaOD, when all the bilirubin dissolves. Such samples could be stored in the dark, at 4°C, for at least days without the occurrence of bilirubin photodegradation.

For the fluorescence and CD experiments the final concentration of bilirubin used was always less than 1×10^{-5} M. 1 cm pathlength cuvettes were used for the fluorescence experiments, while for the CD experiments a 5 cm pathlength, cylindrical cell was employed. Fluorescence studies were carried out on Perkin Elmer MPF **44A** and Hitachi 650–60 fluorimeters and CD studies on a JASCO J20 spectropolarimeter.

Gel permeation studies were done on a Sephadex G-50 column of dimensions 1·1 cm × 70 cm. Blue dextran (Sigma) was used to check the column packing as well as to determine the void volume. The column was calibrated using proteins like melittin (monomeric), cytochrome c from horse heart and ovalbumin. The sample volume loaded varied between 150 and 300μl. In the case where ^{1}H NMR spectra of column fractions are reported, the appropriate fractions were pooled, lyophilized and redissolved in D_2O.

^{1}H NMR spectra were recorded on a Bruker WH-270 FT NMR spectrometer at the Sophisticated Instruments Facility, Indian Institute of Science, Bangalore. No external standard was added to the sample, the 4·76 ppm resonance of H_2O (in D_2O) was taken as an internal reference. All experiments were done at 293 K. Difference nuclear Overhauser effect (NOE) spectra were obtained by sequential recording of perturbed and normal spectra (8 K memory each) using low power on-resonance shifting of the irradiation frequency, respectively. A delay time of 3·0 sec was used between transients. The difference free induction decay was multiplied by a decaying exponential, prior to Fourier transformation.

3. Results

The linear structure of bilirubin IX α, the physiologically important bilirubin isomer, is shown in figure 1. Also shown in figure 1 is the structure of cholate, the

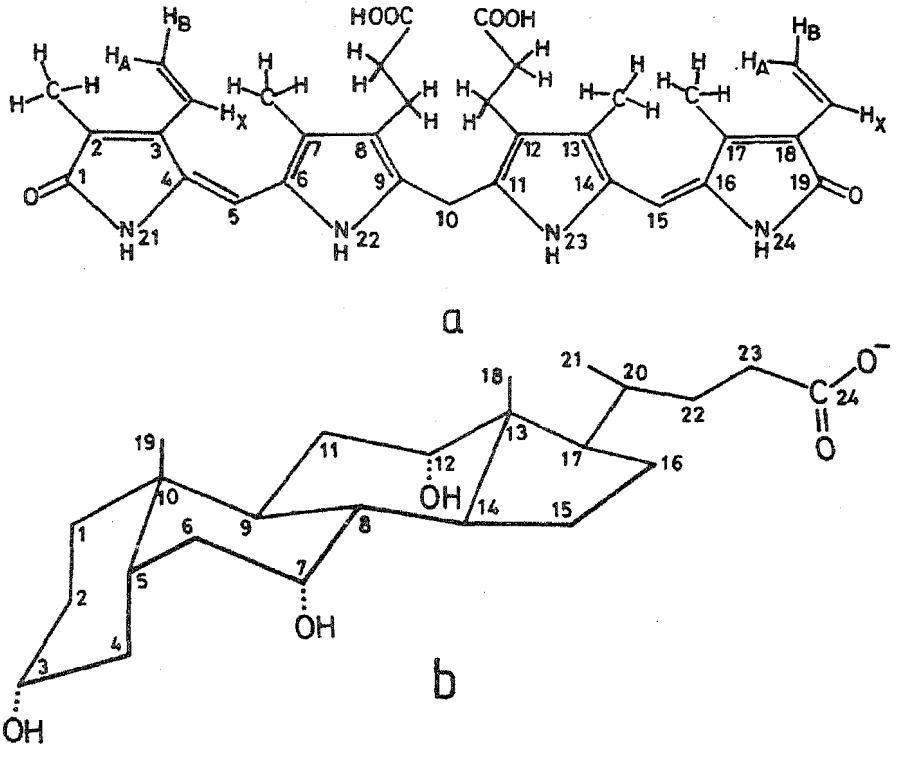

Figure 1. (a) Structure of bilirubin IX α (42, 15Z configuration) with numbering scheme. **(b) Structure** of cholate **with** numbering scheme.

bile salt which **is** the subject of most of the studies described in this report. The other bile salts studied are deoxycholate which lacks a hydroxyl group at position 7 and dehydrocholate, where all the three hydroxyl **groups** are replaced by keto groups.

3.1 *Fluorescence*

Figure 2 shows the enhancement of bilirubin fluorescence in the presence of sodium cholate. Bilirubin is practically non-fluorescent in solution at room temperature, the quantum yield being less than 10^{-4} (Matheson *et al* 1975). Binding to serum albumin results in fluorescence enhancement. This increase has been attributed to translational and vibrational immobilization **of** bilirubin in its bound form (Beaven *et al* 1973). Bilirubin **has also** been shown to exhibit enhanced fluorescence when it binds to gramicidin *S* (Marr-Leisy *et al* 1985) and symmetrical alkyl diamines (Lahiri and Balaram 1987). Increase of bilirubin fluorescence in the presence of other macromolecules can thus be considered as indicating interaction leading to binding. It is interesting to note in figure **3** that the enhancement of bilirubin fluorescence in the presence of varying concentrations of cholate exhibits a sharp discontinuity around **13** mM, fallowed by a further rise. The critical micelle concentration (CMC) of cholate **is** known to be between 11 and **13** mM (Roda *et al* 1983), depending on the presence of salts like sodium chloride. It thus appears that bilirubin binds preferentially to micelles **of** cholate, There is no observed increase in the fluorescence of bilirubin in the presence of the other bile salts, deoxycholate and dehydrocholate. While the CMC of deoxycholate is $\backsim$ 10 mM, that of dehydrocholate is $>$ 250 mM (Roda *et al* **1983).**

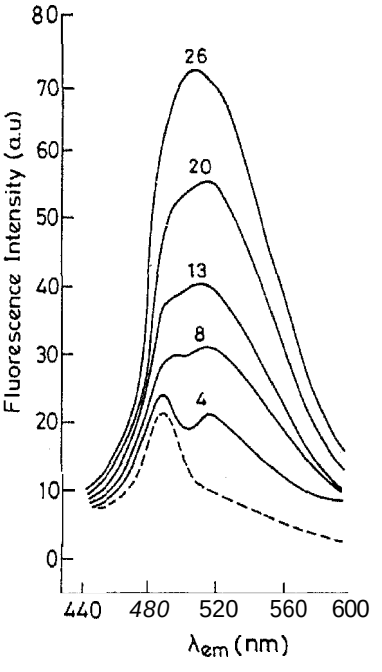

Figure 2. Enhancement of bilirubin ($4{\cdot}8 \times 10^{-6}$ M) fluorescence (arbitrary units) in the presence **of** cholate in H_2O at pH 10.9, 150 mM NaCl. Number over each trace indicates the cholate concentration in mM $\lambda_{ex} = 420$ nm.

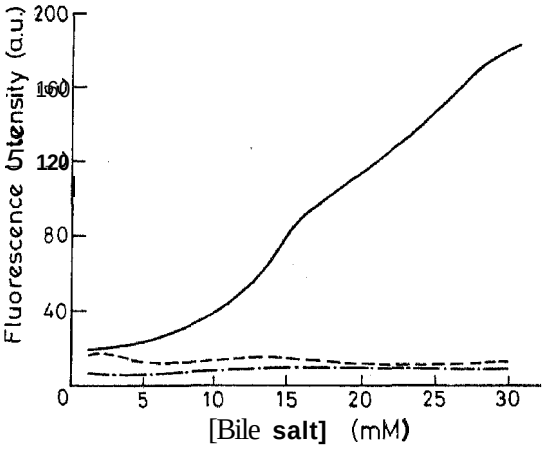

Figure 3. Dependence of bilirubin fluorescence on the concentration of bile salts in H_2O, pH 10.8, 150 mM NaCl. $\lambda_{ex} = 420$ nm, $\lambda_{em} = 520$ nm. (—— 4.6×10^{-6} M bilirubin in cholate; – – – 7.3×10^{-6} M bilirubin in deoxycholate; –·– 7.3×10^{-6} M bilirubin in dehydrocholate.)

3.2 Circular dichroism

CD is a useful technique to monitor bilirubin binding to other molecules since the observation of induced optical activity in the otherwise optically inactive bilirubin is a positive indication of the occurrence of such interactions (Blauer 1983). Such induced optical activity is observed when bilirubin binds to proteins like serum albumins (Brodersen 1982), ligandin (Bhargava *et al* 1980), arninoazodye-binding protein **A** (Tipping *et al* 1976) and chymotrypsin and lysozyme (Blauer 1986). Bilirubin also exhibits induced CD when bound to chiral amines and basic

polypeptides like poly-L-lysine, melittin and gramicidin S (Marr-Leisy *et al* 1985). Induced optical activity has been observed for bilirubin in the presence of sodium deoxycholate (Perrin and Wiisey 1971). Figure 4 shows the induced CD in $7{\cdot}6 \times 10^{-6}$ M bilirubin in the presence of 2×10^{-2} M cholate, deoxycholate and dehydrocholate at pH 10.5. The characteristic bisignate CD pattern is observed with long wavelength positive and short wavelength negative bands, reminiscent of the bilirubin-human serum albumin 1:1 spectrum at ~pH 7 (Blauer and Harmatz 1972). In the case of bile salts, the long wavelength bands lie between 450 and 470 nm and the short wavelength band between 375 and 400 nrn. The CD parameters for bilirubin in the presence of various bile salts are summarized in table 1. The parameters for bilirubin-human serum albumin are also given for comparison. Figure 5 shows the induced CD spectra for bilirubin in presence of increasing concentrations of cholate. The cholate concentrations studied range from 1 to 20 mM. Figure 6 shows a plot of the CD band intensities at 400 and 455 nm as a function of cholate concentration. The results suggest that induced optical activity is detectable even at premicellar cholate concentrations.

3.3 Gel permeation chromatography

To characterize the **size** of the complex formed by bilirubin and cholate, gel permeation Chromatography was performed on a Sephadex *G-50* column. **A** 4:1 ,chelate-bilirubin mixture in water at pH 10·5 was loaded on the column, the eluant

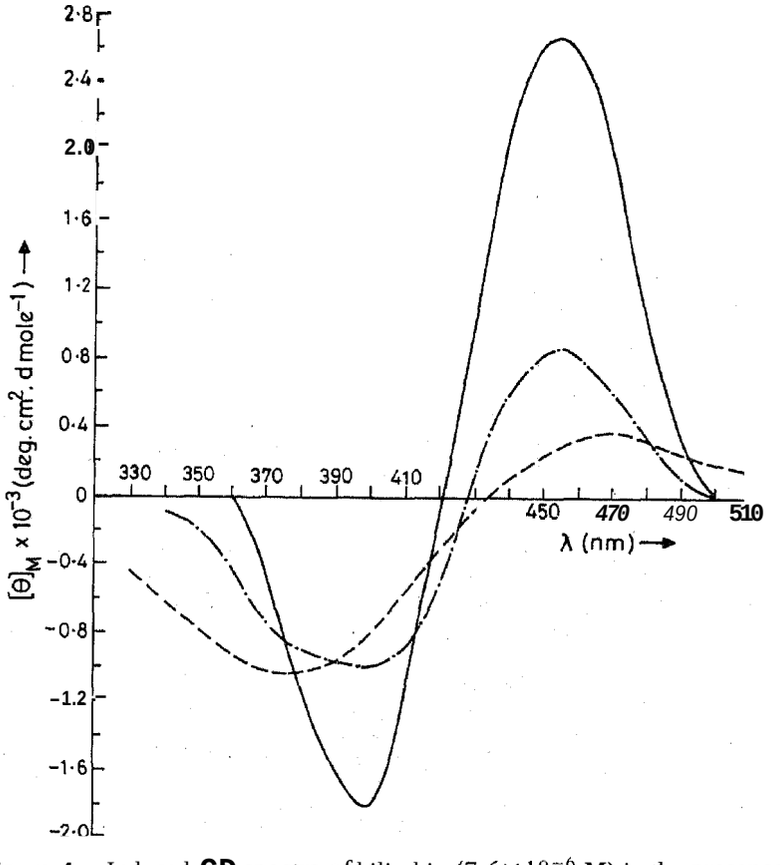

Figure 4. Induced **CD** spectra of bilirubin ($7{\cdot}6 \times 10^{-6}$ **M)** in the presence of 20 mM **bile** salts in H_2O, pH ~ 10·5, 150 mM NaCl. Cholate (—·—), deoxycholate (— – —), dehydrocholate (—)—

Table 1. CD spectral parameters of bilirubin in presence of bile salts.

Bile salt (serum albumin)[a]	Solvent	Bile salt (HSA) concentration (M)	Bilirubin concentration (M)	λ_{nm} ($[\theta]_M$)[b]
Cholate	H_2O, pH 10·6	2×10^{-2}	$7{\cdot}63\times10^{-6}$	400($-1{\cdot}0\times10^3$); 455($0{\cdot}86\times10^3$)
Deoxycholate	H_2O, pH 10.5	2×10^{-2}	$7{\cdot}68\times10^{-6}$	375($-1{\cdot}04\times10^3$); 472($0{\cdot}38\times10^3$)
Dehydrocholate	H_2O, pH 10·5	2×10^{-2}	$7{\cdot}68\times10^{-6}$	398($-1{\cdot}82\times10^3$); 453($2{\cdot}66\times10^3$)
WSA	H_2O, pH 8·7	$3{\cdot}46\times10^{-5}$	$3{\cdot}46\times10^{-5}$	397($-1{\cdot}45\times10^5$); 448($1{\cdot}97\times10^5$)

[a] Data taken from Marr-Leisy *et al* 1985; [b] $[\theta]_M$ values as deg. cm^2. d mole^{-1}.

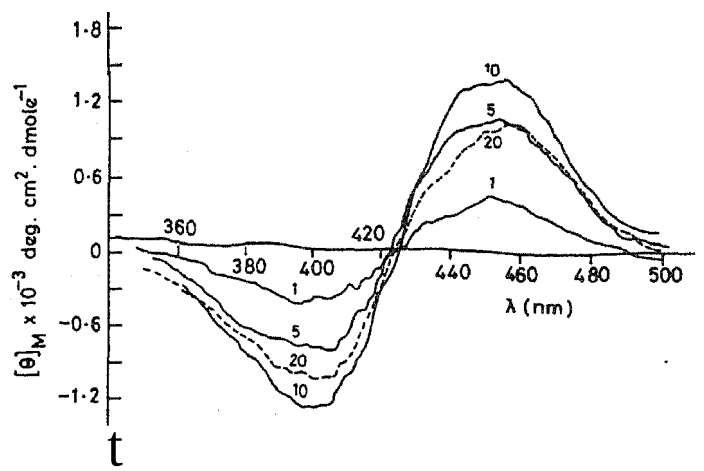

Figure 5. Induced CD spectrum of 6.9×10^{-6} M bilirubin with increasing cholate concentrations in H_2O at pH 9·2 150 mM NaCl. Number over each trace is the concentration of cholate in mM.

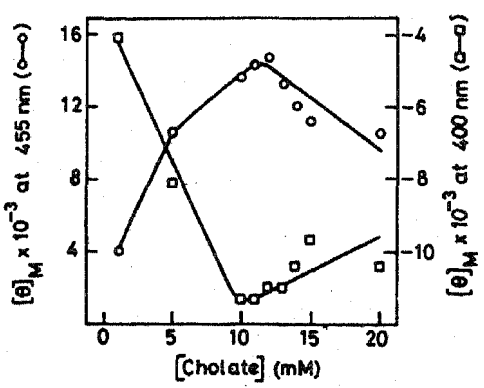

Figure 6. Change in molar ellipticity ($[\theta]_M$) of the bilirubin CD bands at 400 and 455 nm as a function of cholate concentration. ($[\theta]_M$ values as deg. cm^2. dmole^{-1}).

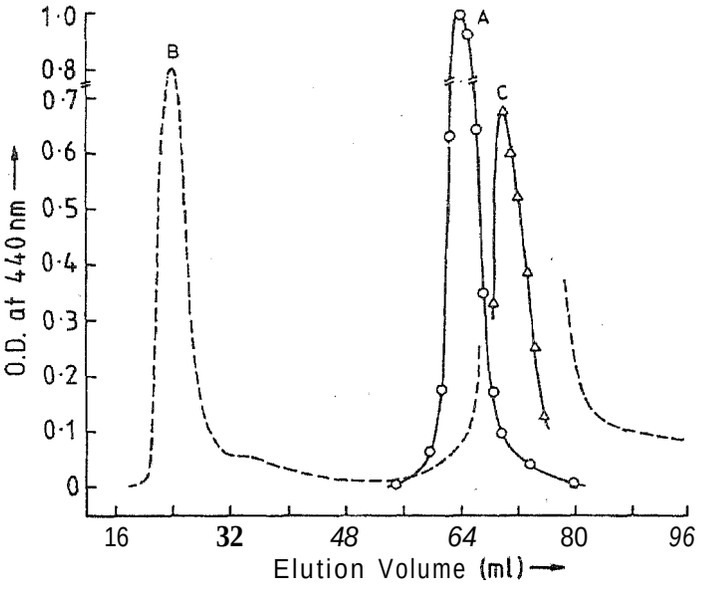

Figure 7. Elution **profiles** of 15 mM bilirubin in **60** mM cholate, pH 10·5 through a Sephadex G-50 column. Peak A is obtained when the eluant is H_2O **at** pH 10·8. **Peaks** B **and** C constitute **the** *two* fractions **when** eluant is at pH 6·6. (Absorbanccs of **peaks A** and C' are of diluted samples.)

being water at pH 10·8 or at pH 6·6. The elution profile was found to depend on the the same pH, i.e. alkaline, the elution profile, which is obtained by measuring the absorbance of each fraction at 440 nm, shows a single peak (peak A). On the other hand, when the eluant is at a pH lower than that of the sample loaded, two well-separated peaks (designated as peaks B and C in figure 7) are observed. Peak B which is almost at the void volume of the column must be a relatively high molecular weight fraction (Sephadex G-50 has an exclusion molecular weight of ~30,000). A cholate solution of similar concentration (60 mM) **was** also run on the same column under identical conditions. The elution profile of cholate, shown in figure 8, does not depend on the pH of the eluant and coincides with the position of peak **A.** To estimate the molecular weights of the column fractions, the column was calibrated using standard proteins and a calibration curve obtained (figure 8 inset). From this curve, the molecular weights of the peaks **A** and C work out to be ~1780 and ~1120, respectively.

These column fractions were subjected to CD studies and analysed for their composition using ^{1}H NMR. For the CD spectra, small aliquots were taken from the desired fraction, diluted **in** water and its pH adjusted before recording the spectrum. The CD data are summarized in figure 9. It is observed that for peak **A,** there is no optical activity at a pH of 11·4. At pH 6·7, weak bands appear, which are stronger at pH 2·7. On the other hand, for peak B, CD spectra are observed at both neutral, as well as alkaline pH. Peak C exhibits a CD spectrum at neutral pH but not at alkaline pH. **As** compared to the CD spectrum of peak B, that of peak C is less intense and has its long wavelength band red-shifted, while its short wavelength band is blue-shifted.

The ^{1}H NMR spectrum of peak **A** was found to be identical to that of the bilirubin:cholate 1:4 sample, i.e., the sample which is loaded on the column.

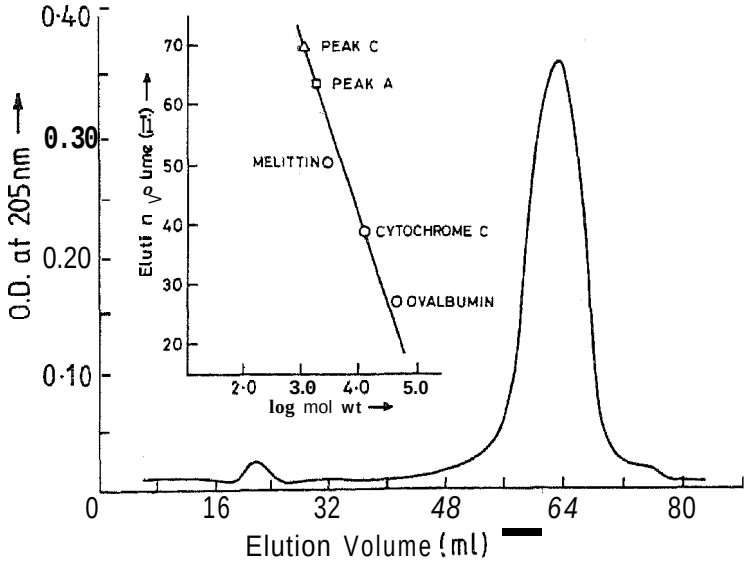

Figure 8. Elution profile of 60 mM cholate through the Sephadex G-50 column. Inset shows the calibration curve, for estimation of molecular weights, of the column using standard proteins. Marked on this are the peak positions of peaks **A** and C.

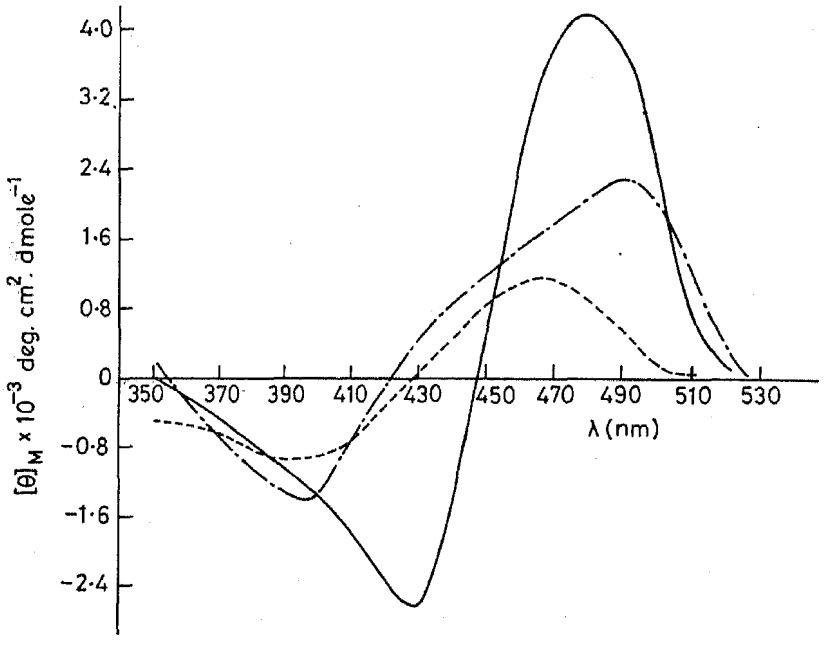

Figure 9. CD spectra of the column fractions. (— — —) peak **A,** pH 2·7, $7{\cdot}45 \times 10^{-6}$ M bilirubin; (——) peak B, pH 6.7, $5{\cdot}76 \times 10^{-6}$ M bilirubin; (— — —) peak C, pH 6.7, 4.4×10^{-6} M bilirubin.

Figure 10 shows this spectrum along with some of the main assignments. The assignment of the cholate peaks between 0·7 and 4·0 ppm is taken from Waterhous *et al* (1985), while that of bilirubin in the region 5 and 7 ppm was obtained from decoupling experiments. Integration of the bilirubin and cholate resonances permits an estimate of the stoichiometry of the bilirubin-cholate complex.

Figure 11 shows the ^{1}H NMR spectrum of peak C. Integration of the bilirubin and cholate resonances establishes that the ratio of bilirubin to cholate is 2: 1, which

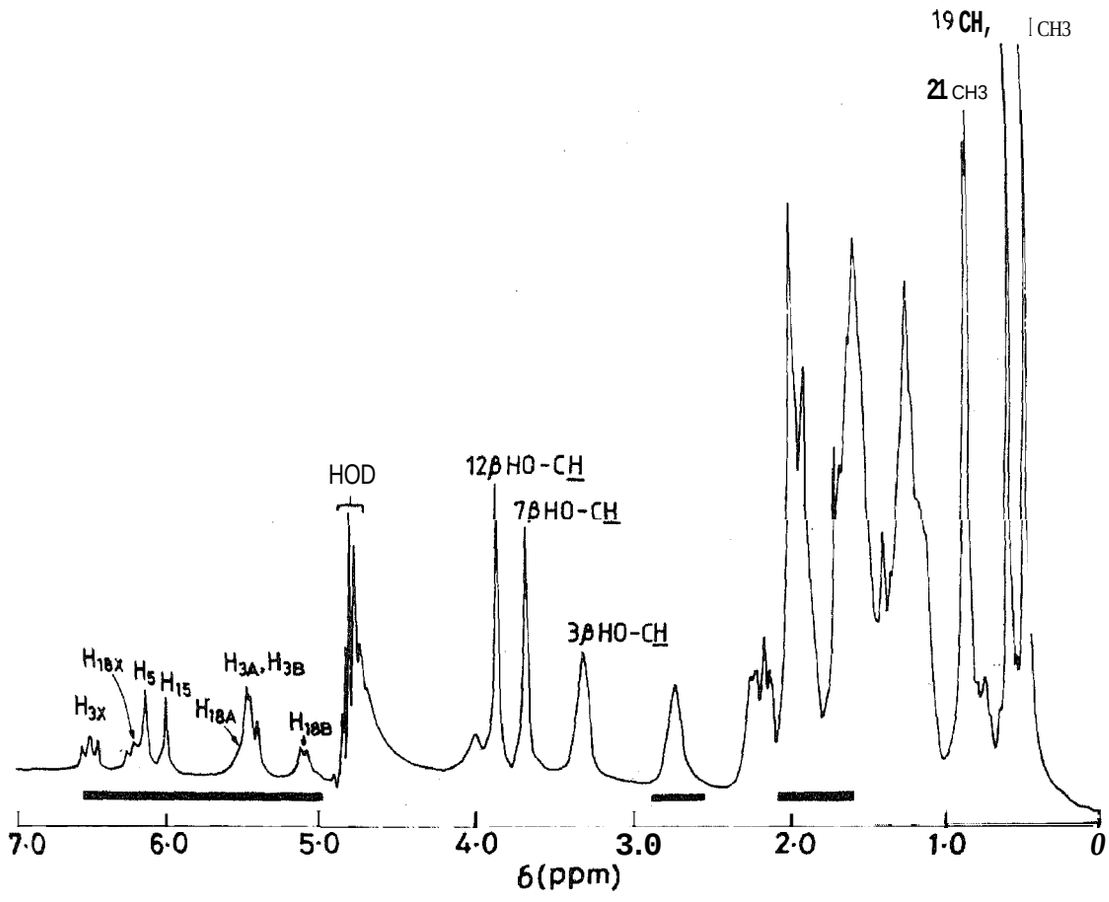

Figure 10. 270 MHz ^{1}H NMR spectrum of 4:1 rholate-bilirubin (120 mM cholate, 30 mM bilirubin) in D_2O at pH 10.5. Major assignments are shown; the shaded zone indicates the region of bilirubin chemical shifts.

is distinctly different from the composition of the mixture loaded on the column, viz., 1:4 bilirubin:cholate. This is not surprising in itself since peak B obviously corresponds to a large complex with a high cholate to bilirubin ratio, suggesting disproportionation of the original 1:4 bilirubin:cholate mixture.

3.4 *Nuclear Overhauser effects*

The precise nature of intermolecular interactions can, in principle, be probed by the use of nuclear Overhauser effects (Bothner-By 1979). Spatial proximity of protons (hydrogen atoms) can generally be established for interproton distances of < 3Å. In the case of macromolecular and micellar systems the sign of the observed NOE are dependent on the product of the Larmor precession frequency (w) and rotational correlation time (τ_c), with positive NOE observed for $\omega\tau_c < 1$, while negative NOE are observed for $\omega\tau_c > 1$ (Bothner-By 1979). Thus, NOE also provide a means of estimating τ_c values which in turn can be related to the molecular size.

One-dimensional NOE measurements were performed on the 1:4 bilirubin:cholate system. Figure 10 shows the 270 MHz ^{1}H NMR spectrum of a 1:4 mixture of bilirubin and cholate. The olefinic proton resonances of bilirubin are confined to

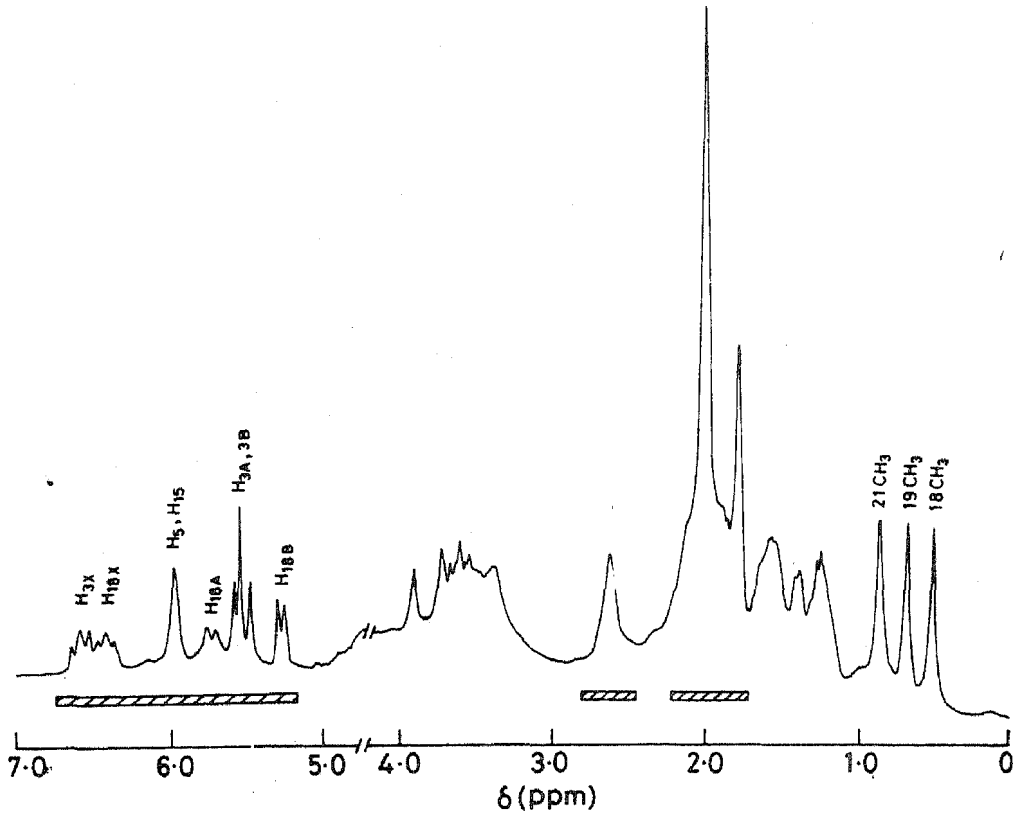

Figure 11. 270 MHz ^{1}H NMR **spectrum of peak C in** D_2O, **pH** 11·5. **Specific assignments are indicated. The hatched region corresponds to** bilirubin **resonances.**

the low field region between 5 and 6.7 ppm. The methyl resonance corresponding to the $-CH_3$ groups at positions 2, 7, 13 and 17 lie between 1·7 and 2·1 ppm. The propionate $-CH_2$ protons appear at 2·74 ppm. These resonances are marked by a hatched line in figure 10. **All** the steroid proton resonances of cholate are limited to the spectral region between 0·5 and **4 ppm.**

Figure 12 shows the results of representative NOE experiments on the **1:4** bilirubin-cholate mixture. Besides the expected intramolecular NOE, some intermolecular, bilirubin to cholate, NOE are also observed. For example, in figure 12b irradiation of the bilirubin olefinic methyl resonances clearly shows the expected intramolecular NOE on the H_5 and H_{15} methine protons. The proximity of these protons is not clearly evident from the linear structure shown in figure 1a. However, it should be noted that rotation about the C_5–C_6 and C_{14}–C_{15} **single** bonds brings these atoms into close proximity. NOE are also observed on the H_{12}, H_7 and H_3 protons of the steroid. These NOE can be rationalized **as** intramolecular cholate NOE, since the $H_{2\beta}$, $H_{11\alpha}$, $H_{11\beta}$ and $H_{6\beta}$ protons have been assigned to resonances in this region (Waterhous *et al* 1985). The spectrum in figure 12c illustrates the effect of irradiating the C_{19} methyl group of, cholate. Two strong NOE are observed on the cholate protons $H_{12\beta}$ and $H_{7\beta}$. While the NOE on $H_{12\beta}$ can be rationalized as an intramolecular effect due to partial saturation of the proximate C_{18} methyl group, the observed NQE on $H_{7\beta}$ can only be interpreted in terms of an ***intermolecular*** cholate-cholate NOE arising from an aggregated species. **An** examination of the perspective diagram of cholate in figure 1b

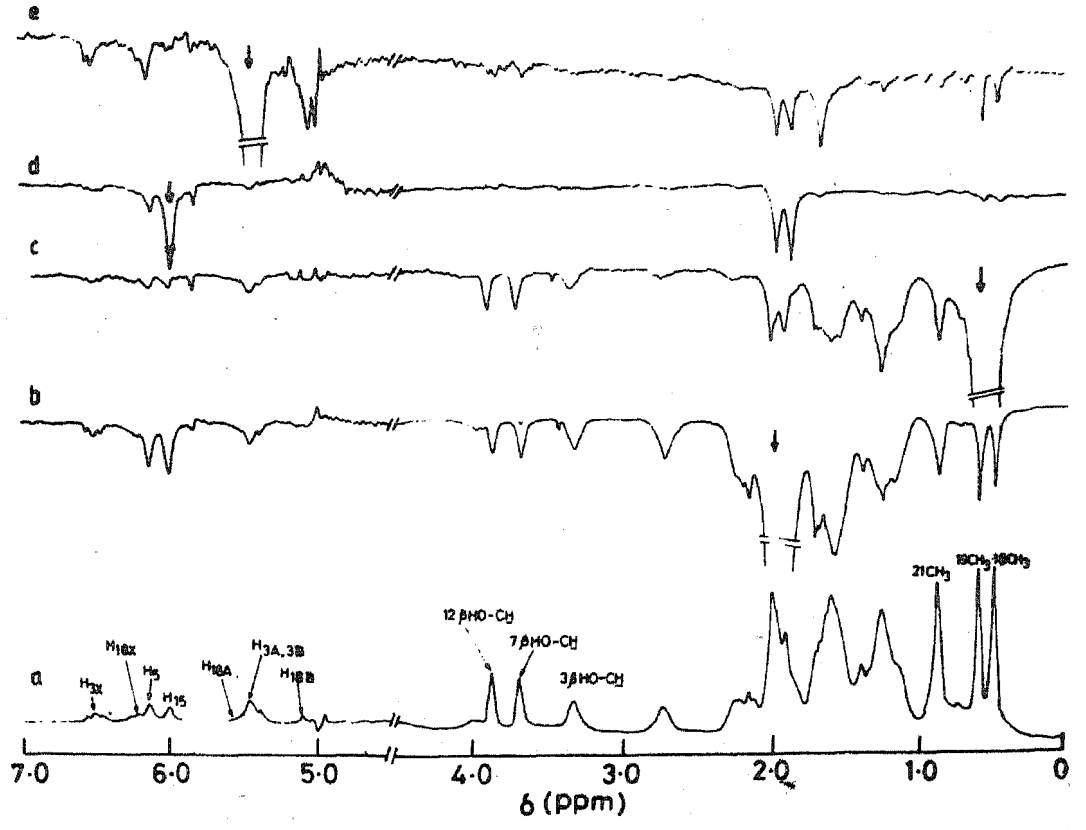

Figure 12. (a) 270 MHz ^{1}H NMR spectrum of 4:1 cholate-bilirubin. **(b–e)** Difference NOE spectra obtained **upon** irradiation of **the** resonances indicated by an **arrow.** The difference NOE spectra were obtained **as** mentioned in the **text** and **are** magnified by a factor of 8. (Bilirubin concentration, **30** mM; cholate, 120 mM.)

establishes, that the $H_{7\beta}$ cannot be spatially proximate to either the C_{18} or C_{19} methyl **groups.** Irradiation of the H_{15} resonance of bilirubin (figure 12d) results in two clear NOE at 1.91 and 2·01 ppm These correspond to the methyl groups at C_{13} and C_7 of bilirubin. Figure 12e **shows** the result of an experiment when the olefinic protons on bilirubin, H_{18A} and H_{3A}, were irradiated. Irradiation of these resonances is expected to lead to NOE on the methyl groups at C_2 and C_{17} of bilirubin. In addition rotation of the vinyl **group** at position 3 can result in an NOE to the C_7 methyl group also. Indeed, NOE to three bilirubin methyl groups are observed at 1·73, 1·91 and 2·01 ppm. **A** most interesting feature of figure 12e **is** the observation of NOE on the C_{18} and C_{19} methyl groups of cholate when the H_{3A} and H_{18A} protons of bilirubin are irradiated. **A** comparison of figures 12b and 12e clearly shows that this is a selective NOE, since no such effect **is** observed when H_{15} of bilirubin is irradiated. Thus the spectrum in figure 12e provides clear evidence for an intermolecular interaction between bilirubin and cholate, which brings specific, peripheral olefinic protons into close proximity with the projecting methyl groups on the cholate surface.

All the NOE observed in this study are negative. The magnitudes observed fall in the range 5 to 20%. This suggests that the cholate-bilirubin complex lies in the long correlation limit with $\omega\tau_c > 1$. For molecules of the size of bilirubin or cholate, monomeric species axe expected to yield positive NOE at **270** MHz. Indeed

positive NOE have been observed in earlier NMR studies of pure bilirubin in chloroform (Kaplan and Navon 1981) and pure cholate in water below the CMC (S Raghothama, unpublished results). The observation of negative NQE provides further support for the presence of aggregated species in solution for the 4:1 cholate-bilirubin mixture.

4. Discussion

The interaction of bilirubin with bile acids may be monitored by a variety of spectroscopic techniques. As demonstrated in the present study, fluorescence, CD and NMR methods can be useful in probing bilirubin-cholate interactions. While the observation of spectral changes in the presence of bile salts provides support for an intermolecular interaction, the precise nature of the interacting species is less evident. The absence of detectable spectral changes cannot be taken as evidence for the absence of intermolecular interactions.

These features are clearly illustrated by considering the results of the fluorescence and CD studies in conjunction. In the case of cholate a strong enhancement of bilirubin fluorescence is observed at the CMC of cholate (figure 3). The observation of induced CD bands, however, occur at significantly lower cholate concentrations, with appreciable optical activity even at premicellar Concentrations (figure 5). In this case it appears that fluorescence enhancements accompany micellar solubilization of bilirubin, whereas induced optical activity results even in the case of presumably low molecular weight complexes. Induced optical activity is also observed upon addition of steroid derivatives like dehydrocholate, which is known to be incapable of micellar aggregation at the concentrations used in this study (Roda *et al* 1983). Deoxycholate, which is known to form micelles at concentrations above 10 mM, causes induced optical activity of bilirubin but does not yield a fluorescence enhancement. It is likely that the nature of cholate and deoxycholate micelles may be different leading to a greater conformational flexibility of the bilirubin molecule in the case of the latter. This could lead to enhanced vibrational deexcitation in the deoxycholate case, resulting in a quenching of fluorescence (Braslavsky *et al* 1983).

The gel permeation studies described earlier afford a means of estimating the size of the micellar complexes under observation and also permit evaluation of the effect of pH on the stability of these cbmplexes. The 1:4 bilirubin-cholate mixture (15 mM bilirubin, 60 mM cholate) used in the gel permeation studies was prepared at pH 10·5, to facilitate dissolution of bilirubin at such high concentrations. 'Under these conditions, optically clear, intensely absorbing solutions were obtained. Elution profiles were obtained on a Sephadex G-50 column under two distinctly different pH conditions, viz., pH 6.6 and 10·8. The characteristics of the various bilirubin-cholate fractions are summarized in table **2.** While two distinct fractions (pegks B and C) are obtained at neutral pH, only one peak **(A)** is obtained. when the elution is performed at alkaline conditions.

Peak **A** corresponds to a molecular weight of ~ 1780 and from an integration of the ^{1}H NMR spectrum a cholate to bilirubin stoichiometry of **4: 1** is obtained. This species may thus be assigned to a relatively small mixed aggregate composed of approximately 3 to **4** cholate molecules and one bilirubin molecule. Under similar

Table 2. Characterization of bilirubin-cholate complexes obtained by gel permeation.

Fraction	Stoichiometry cholate:bilirubin	Estimated molecular weight	CD parameters at different pH values			NOE	
			Acidic $\lambda_{nm}([\theta]_M)^a$	Neutral $\lambda_{nm}([\theta]_M)$	Alkaline $\lambda_{nm}([\theta]_M)$	Intra-molecular	Inter-molecular
Peak A	4:1	~1780 (1805–2212)[b]	395(-0.9×10^3); 465(1.1×10^3)	397(-0.5×10^3); 440(0.4×10^3)	c	Observed (negative)	Observed (negative)
Peak B	Cholate 4 bilirubin	≥ 30000	d	430(-2.6×10^3); 480(4.2×10^3)	435(-2.8×10^3); 495(2.5×10^3)	Not determined	Not determined
Peak C	1:2	~1120 (1575)	d	397(-1.5×10^3); 490(2.3×10^3)	c	Observed (Negative)	Not (observed)

[a] $[\theta]_M$ values as deg.cm^2.dmol^{-1};
[b] values in parentheses correspond to molecular weights for the 3:1 and 4:1 cholate:bilirubin complexes in rhe case of peak A and the 1:2 complex for peak C;
[c] no spectrum observed;
[d] not determined.

elution conditions 60 mM cholate eluted at exactly the same position (figure 8). This would correspond to a primary cholate micelle with an aggregation number of approximately 4 to 5. This is in general agreement with estimates of primary micelle size for bile salts which suggest aggregation numbers between 2 and 10 molecules (Carey and Small 1972). It is likely that the mixed aggregate corresponding to peak A results from incorporation of a single bilirubin molecule into the primary micelle. Under the conditions used in this study, a clear resolution of the differences in aggregate size between the pure primary cholate micelle and mixed micelle cannot be made.

The CD spectrum of peak A shows a remarkable sensitivity to the pH of the medium. While characteristic exciton split bilirubin CD profiles are observed at pH 2·4 and 6·7, no induced CD spectrum is detected at alkaline pH. It is likely that in the low molecular weight aggregate, bilirubin is relatively more exposed to the solvent environment at pH 11·4. The absence of CD bands can then be due to conformational flexibility or due to equal populations of both right- and left-handed chiral forms. At lower pH, the structure of the aggregate may be distinctly different with bilirubin now occupying a more sequestered position. Under these conditions, chiral perturbations are more likely to result in an induced CD spectrum. Exactly similar CD behaviour was observed for a 4:1 cholate:bilirubin mixture, which had not been subjected to gel filtration. NOE studies of peak A yielded both intra and intermolecular NOE similar to those described for the 4:1 cholate: bilirubin mixture.

A sudden drop in pH, when the eluant is at pH 6·7, results in a fragmentation of the mixed bilirubin-cholate micelles. A marked pH dependence has also been observed in the bilirubin-human serum albumin case (Brodersen 1982) which has been attributed to the presence of a second type of bilirubin-albumin complex. This complex, which is different from the 1:1 complex, is a large aggregate of bilirubin acid and albumin in molar proportions of about 300:1. Such aggregates can be dissolved on addition of sodium hydroxide, and they leave a 1:1 complex and an excess of bilirubin dianion in solution.

It seems that a similar process is taking place in the bilirubin-cholate case too, with the formation of a 2:1 complex (bilirubin:cholate), and a large complex, which elutes in the void volume of the column and which has very little bilirubin solubilized in a large micellar cholate aggregate.

The stoichiometry of the complex corresponding to peak C is unambiguously established by its proton NMR spectrum (1:2 cholate :bilirubin). The estimated molecular weight of ~1120 suggests that this fraction corresponds to a trimeric complex with one cholate and two bilirubin molecules. In this case a characteristic CD spectrum was observed at neutral pH but no optical activity could be detected at alkaline pH. Presumably the trimeric complex readily dissociates at high pH into its individual components. An interesting feature of peak C is the absence of any intermolecular NOE suggesting that the disposition of cholate and bilirubin molecules is appreciably different from that in peak A.

Peak B is undoubtedly a high molecular weight fraction containing a large excess of cholate and can be best described as a micellized bilirubin fraction. In this case induced CD spectra were observed at both neutral and alkaline pH.

In the present study NOE have been used to provide definitive evidence for close intermolecular interactions in the 4:1 cholate:bilirubin system. A particular point

of interest is the observation of relatively large *intramolecular* NOE for both bilirubin and cholate molecules. Earlier studies of bilirubin in organic solvents like chloroform and dimethyl-sulfoxide (Kaplan and Navon 1981, 1982) have yielded limited NH↔ NH NOE between pyrrole NH protons and NH↔ CH NOE between pyrrole NH and the bridging methylene protons. In the present study, several NOE have been observed between the olefinic **protons** of the vinyl group and the bridging methine groups and the peripheral methyl groups. Some of these NOE are in fact conformation sensitive NOE, which provide information about the orientations of the pyrrole groups about the C_5–C_6 and C_{14}–C_{15} single bonds. The observation of these NOE is undoubtedly facilitated by the fact that the complexes have long correlation times, which result in larger magnitudes of the cross relaxation parameters.

A more extensive analysis of the observed NOE together with the CD results may provide a greater insight into the conformations of bilirubin packaged into cholate aggregates.

Acknowledgement

We thank S Raghothama for carefully performing the difference NOE experiments.

References

Beaven G H, d'Albis A and Gratzer W B 1973 *Eur. J. Biochern.* **33** *500.*
Bhargava M M, Ohmi N, Listowsky I and Arias M I 1980 *J. Biol. Chem.* ***255*** 718
Bickel M H and Minder R 1970 *Biochem. Pharmacol.* **19** 2437
Blauer *G* 1983 ***Israel*** *J. Chem.* **23** 201
Blauer G 1986 *Biochim. Biophys. Acta* **884** 602.
Blauer *G* and Harmatz D 1972 *Biochim. Biophys. Acta* **278** 89
Bothner-By A A 1979 in ***Magnetic*** *resonance* ***in biology*** (ed.) R G Shulman (New York: Academic Press) **p.** 177
Braslavsky S E, Holzwarth A R and Schaffner K 1983 ***Angew.*** *Chem., Int.* ***Ed.*** *Engl.* 22 656
Brodersen R 1982 in ***Bilirubin*** (eds) K P M Heirwegh and S B Brown (Boca Raton, Fl: CRC Fress) vol. 1, **p.** 75
Brown S B and Troxler R F 1982 **in** *Bilirubin* **(eds)** K P M Heirwegh and S B Brown (Boca Raton, Fl: CRC Press) vol. **2,** p.1
Carey M C and Koretsky A P 1979 *Biochern. J.* **179** 675
Carey M C and Small D M 1972 *Arch. Intern. Med.* **130** 506
Goresky C A, Naddad H H, Kluger W S. Nadeau B E and Bach G G 1974 Can. *J. Physiol. Pharmacol.* **52** 389
Kaplan D and Navon G 1981 *J. Chem.* ***Sac.*** *Perkin II* **1374**
Kaplan D and Navon G 1982 *Biochem* ***J.*** **201** 605
Lahiri K **and** Balaram P 1987 *J. Biosci.* **11** 485
Marr-Leisy D, Lahiri K and Balaram P 1985 *Int.* ***J.*** *Pept. Protein Res.* **25** 290
Matheson I B C, Faini G J and Lee 3 *3975 Photochem. Photobiol.* **21** 135
McDonagh A F and Assisi F 1972 *Biochem. J.* **129** ***797***
Meuwissen J A T P and Heirwegh K P M 1982 in ***Bilirubin*** (eds) K P M Heirwegh and ***S*** B Brown (Boca Raton, Fl: CRC Press) vol. 2, **p.** 39
Ostrow J D and Celic L **1984** *Hepatology* **4 385**

Perrin J H and Wilsey M 1971 J. ***Chem.*** *Soc., Chem. Commun.*769
Reuben **A** 1984 *Hepatology* **4** 212S
Reuben **A,** Howell K E and Boyer J L 1982 *J.* ***Lipid*** *Res.* **23** 1039 .
Roda **A,** Hofmann **A** F and Mysels K J 1983 *J.* ***Biol.*** *Chem.* **258** 6362
Scharschmidt B F and Schmid R 1378 *J. Clin. Invest.* **62** 1122
Tipping E, Ketterer B, Christodoulides L and Enderby ***G*** 1976 *Biochem.* J. **157** 211
Waterhous D **V,** Barnes S and Muccio D D 1985 *J.* ***Lipid*** *Res.* **26** 1068